Crucial Role of the Spacer in Tuning the Length of Self-Assembled Nanorods

Shuaiyuan Han, Gaëlle Mellot, Sandrine Pensec, Jutta Rieger, François Stoffelbach, Erwan Nicol, Olivier Colombani, Jacques Jestin, Laurent Bouteiller

The crucial role of the spacer in tuning the length of self-assembled nanorods

Shuaiyuan Han,[a] Gaëlle Mellot,[a] Sandrine Pensec,[a] Jutta Rieger,[a] François Stoffelbach,[a] Erwan Nicol,[b] Olivier Colombani,[,b] Jacques Jestin[c] and Laurent Bouteiller*[,a]*

[a] Sorbonne Université, CNRS, Institut Parisien de Chimie Moléculaire, UMR 8232, Equipe Chimie des Polymères, 75252 Paris, France

[b] Institut des Molécules et Matériaux du Mans (IMMM), UMR 6283 CNRS Le Mans Université, Avenue Olivier Messiaen, 72085 Le Mans Cedex 9, France

[c] Laboratoire Léon Brillouin, UMR12 CEA-CNRS, Bât. 563, CEA Saclay, 91191 Gif-sur-Yvette, France

ABSTRACT. Polymeric supramolecular nanorods were prepared in toluene by self-assembly of tris(urea) stickers connected on both sides through alkyl spacers of different lengths to short poly(styrene) (PS) arms. Several tris(urea) initiators or chain transfer agents were synthesized straightforwardly and used to grow well-defined PS arms *via* Atom Transfer Radical Polymerization (ATRP) or Reversible Addition Fragmentation chain Transfer (RAFT) polymerization. Self-assembly was investigated by means of FTIR and light/neutron scattering. A dramatic impact of the spacer separating the tris(urea) sticker from the PS arms on the extent of self-assembly was observed in toluene as long as the degree of polymerization of the PS arms (x) was kept short (x ~ 10). Indeed, supramolecular nanorods of several hundreds of nm in length for

a few nm in radius were obtained with a spacer consisting of 9 atoms, whereas 5 times shorter nanorods were obtained for a spacer of only 5 atoms, and spherical particles were found in the absence of any spacer, all other parameters remaining unchanged. These results reveal the possibility to tune the length of polymer-decorated supramolecular nanorods with minimal modification of the assembling sticker and without affecting the functionality of the rods.

INTRODUCTION

One-dimensional nanomaterials (*e.g.* nanorods) exhibit many interesting properties and applications due to their large specific surface area and shape anisotropy[1] such as: colloidal semi-conductor,[2] active materials of batteries,[3] (bio)sensing,[4] nanomedicine,[5] catalysis,[6,7] soft adhesive materials.[8] Because of the anisotropy of nanorods, their electrical,[2] optical,[9] and mechanical properties[10] in the longitudinal and transverse directions exhibit great differences. Of course, the properties and uses of rod-like particles depend on their aspect ratio.[11] For example rod-like nanoparticles are likely to form a liquid crystal phase only when the aspect ratio is large enough.[12]

Self-assembly based on non-covalent bonds is an efficient bottom-up approach to get nanorods[13-15] and one elegant way is to use directional self-assembly of hydrogen bonding stickers.[16-22] In this case, it has been demonstrated that the extent of self-assembly and therefore the length of the rods can be tuned by a) changing the solvent,[18] b) addition of a stopper[23] and c) modifying the sticker.[24,25] Nanorods can be made functional by attaching polymer arms to such a sticker. Moreover, polymer arms increase the number of possibilities to tune the length of the self-assembled rods by: a) altering the chemical nature of the arms,[17,24,26,27] b) introducing stimuli sensitive parts,[27-29] c) changing the number of arms[28] and d) modifying their length.[17,26,30]

However, in all these examples, the influence of the spacer connecting the hydrogen bonding sticker to the polymer arm on the self-assembly has been neglected to the best of our knowledge. Catrouillet et al.[24,26] observed a strong weakening of the self-assembly in cyclohexane of a tris(urea) when it was decorated by polystyrene (PS) arms rather than polyisobutene (PIB) ones. They suggested that this could be due to the fact that the bulky styrene units were directly attached to the tris(urea). Here we report that separating the tris(urea) self-assembling sticker from the first styrene unit by flexible alkyl spacers of different sizes dramatically alters the extent of self-assembly, providing a simple way to prepare supramolecular nanorods with tunable lengths while barely affecting the chemical structure or functionality of the supramolecules. The functional polymers were prepared by ATRP or RAFT polymerization[31,32] and their self-assembly in toluene was investigated by FTIR spectroscopy and light/neutron scattering. Polymer arms with two different degrees of polymerization (DP_n = x = 10 or 30 per arm) were attached to the stickers to discriminate the effect of the length of the polymer arms from that of the spacer on the self-assembly.

EXPERIMENTAL SECTION

Synthesis. The synthesis of polymers L_x, S_x and R_x is described in details in Supporting Information (SI), section 1. That of N_x was previously reported in reference[26] where N_{10} and N_{30} were respectively called $S_{14}U_3S_{14}$ and $S_{34}U_3S_{34}$.

Preparation of solutions. Transparent polymer solutions for light and neutron scattering were obtained by direct dissolution of the polymers at room temperature in toluene or toluene-d_8, respectively. For light scattering, stock solutions were first prepared at 10 g/L and filtered on 0.45 μm filters. More diluted samples (0.25 – 1 g/L) were obtained by dilution of the filtered stock

solutions with toluene filtered on 0.02 μm filters and analyzed as they were. For SANS, polymer solutions were prepared at 10 g/L and measured at this concentration. For FTIR spectroscopy, polymer solutions were prepared by direct dissolution of the polymers at 2.8 mmol/L either in toluene or chloroform.

Light scattering. Measurements were done with a standard ALV-CGS3 system equipped with an ALV-5003 multi tau correlator system (ALV GmbH, Germany) with a vertically polarized helium-neon laser with wavelength λ = 633 nm as light source. The measurements were done at 20°C over a large range of scattering vectors q varying from *ca.* 3×10^{-4} Å^{-1} to 3×10^{-3} Å^{-1}. $q = \frac{4\pi n}{\lambda} \sin\left(\frac{\theta}{2}\right)$, with θ the angle of observation, n the refractive index of the solvent and λ = 633 nm the wavelength of the laser. Details of the treatment of the data are given in SI sections 2.1 and 2.4.

Small Angle Neutron Scattering (SANS). SANS measurements were made at the LLB (Saclay, France) on the PA20 instrument, at sample to detector distances (1.5, 8 and 18.5 m) and wavelengths (4 and 6 Å) to cover the 2.5 10^{-3} to 0.44 Å^{-1} q-range, where the scattering vector q is defined as usual, assuming elastic scattering ($q = (4\pi/\lambda)\sin(\theta/2)$, where θ is the angle between incident and scattered beam). Data were corrected for the empty cell signal, the solute and solvent incoherent background. A light water standard was used to correct the detector inhomogeneities and to normalize the scattered intensities to cm^{-1} units. The data were fitted with the DANSE software SasView.[33] Details of the treatment of the data are given in SI section 2.4.

Fourier Transformed Infrared Spectroscopy (FTIR). Infrared spectra were recorded on a Nicolet iS10 spectrometer. Polymers were dissolved in chloroform (stabilized with methyl butene) or toluene to obtain 2.8 mmol/L solutions. The solutions were measured in 1 mm KBr cells.

RESULTS

Synthesis. Four different series of macromolecules were synthesized consisting of a tris(urea) sticker to which two PS arms were symmetrically connected (Scheme 1, see details of the synthesis in SI section 1). These macromolecules differed by the nature of the spacer connecting the tris(urea) sticker to the PS arms. Moreover, for each series, two different degrees of polymerization (x ~ 10 or 30 per arm) were targeted to discriminate the influence of this parameter compared to that of the spacer on the self-assembly. For N_x, S_x and L_x, containing respectively **N**o-spacer, a **S**hort spacer or a **L**ong spacer, the length of the polymer arms was controlled by ATRP. The spacer used for R_x is very similar to that of L_x but contains a trithiocarbonate moiety, which was used to control the polymerization of styrene by **R**AFT.

The chemical structure of the polymers and the degree of polymerization of the PS arms were confirmed by ^{1}H NMR (Table 1). As shown in Figure 1, SEC revealed that all polymers exhibited consistent molar masses and fairly narrow dispersities, even though some differences exist between the samples: 1) the maximum of the SEC distribution is slightly shifted to smaller molar masses for N_{10} compared to S_{10}, L_{10} and R_{10}, whereas that of L_{30} is slightly shifted to larger molar masses compared to N_{30}, S_{30} and R_{30} and 2) S_x and L_x show a significant tailing towards higher molar masses, and thus their dispersity is significantly higher ($Đ$ ~ 1.4) compared to that of sample R_x (and N_x) ($Đ$ ~1.2, see Table 1).

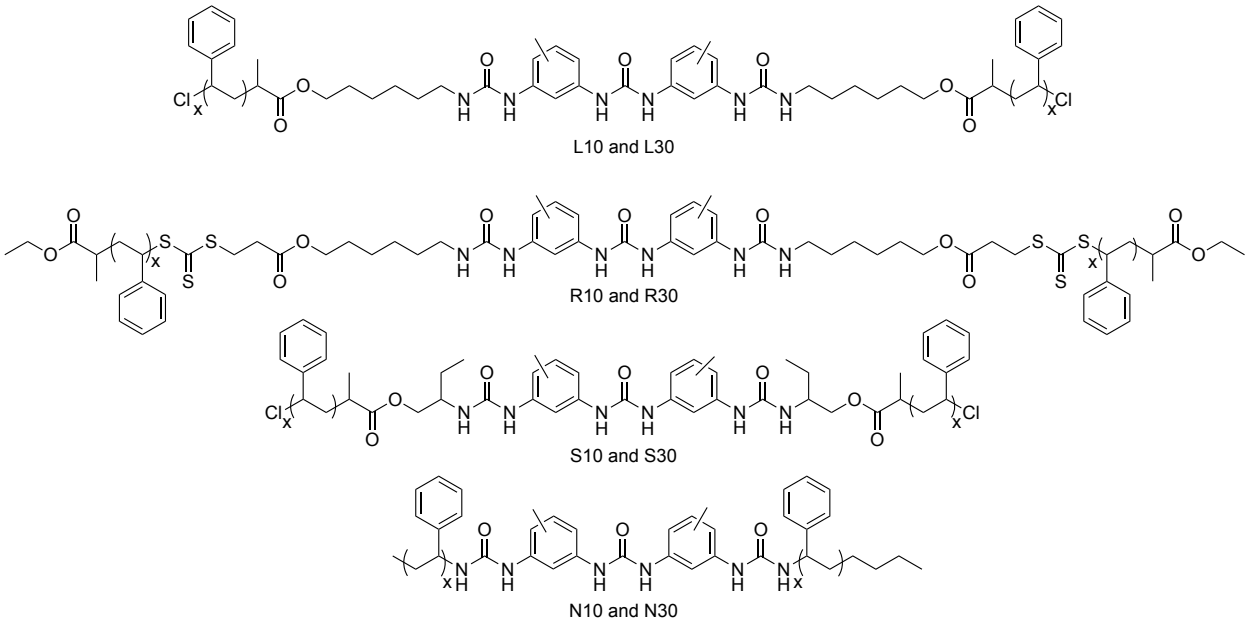

Scheme 1. Structure of L_x, R_x, S_x and N_x.

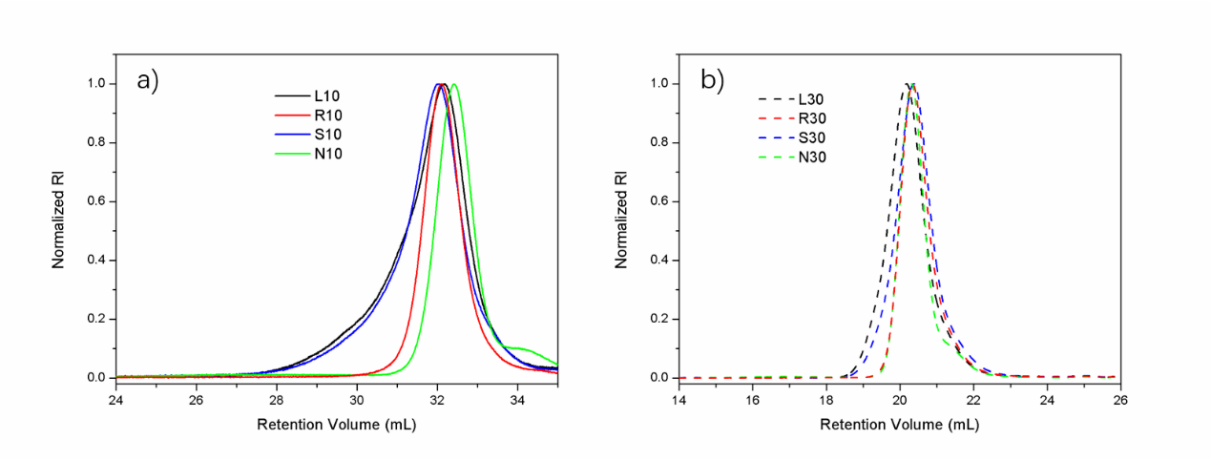

Figure 1. SEC distributions obtained for a) L_{10}, R_{10}, S_{10} and N_{10} in DMF (these samples could not be analyzed in THF because of aggregates formation) and b) for L_{30}, R_{30}, S_{30} and N_{30} in THF.

Table 1. Characterization of the polymers.

Name	$M_{n,th}$ [a] (kg/mol)	$DP_{n,NMR}$ [b]	$M_{n,NMR}$ [c] (kg/mol)	$M_{n,SEC}$ [d] (kg/mol)	$Đ_{SEC}$ [d]
L_{10}	2.6	11	3.1	5.7	1.36
R_{10}	3.7	16	4.4	4.8	1.13
S_{10}	3.1	13	3.3	4.8	1.38
N_{10}	2.7	14	3.5	3.3	1.17
L_{30}	7.0	35	8.0	11.4	1.39
R_{30}	6.9	35	8.3	8.0	1.17
S_{30}	6.9	33	7.5	9.2	1.32
N_{30}	7.0	34	7.6	9.0	1.15

[a] Theoretical M_n at final conversion. [b] Average value per arm, measured by ^{1}H NMR. [c] Measured by ^{1}H NMR. [d] Measured by SEC (see SI section 1.1).

FTIR investigation of the hydrogen bonding ability. FTIR experiments were first conducted in chloroform ($CHCl_3$) which is a moderate hydrogen bond competitor. In this solvent, both a narrow stretching band at ~ 3430 cm^{-1} characteristic of free NH and a broader stretching band at ~ 3300 cm^{-1} characteristic of intermolecularly hydrogen bonded NH were observed for all eight polymers[34] (Figures 2a,b). For x ~ 30 (Figure 2b), the free NH contribution is overwhelming for N_{30}, whereas the bonded NH contribution is much stronger for the three other polymers (L_{30}, R_{30} and S_{30}). These results hint at a much stronger self-assembly in the presence of a spacer. Based on the same reasoning, a drastic enhancement of the self-assembly in the presence of the spacer can also be observed for x ~ 10 (Figure 2a). More precisely, the bonded to free NH ratio (and therefore the extent of self-assembly) increases in the order $N_{10} << S_{10} < R_{10} < L_{10}$. The only important difference between x ~ 10 and x ~ 30 is that for longer arms the fraction of free NH increases

without changing the tendencies observed for x = 10. This influence of the length of the arms is expected,[17,26] and is due to the stronger entropic penalty of stretching for the longer arms.[35]

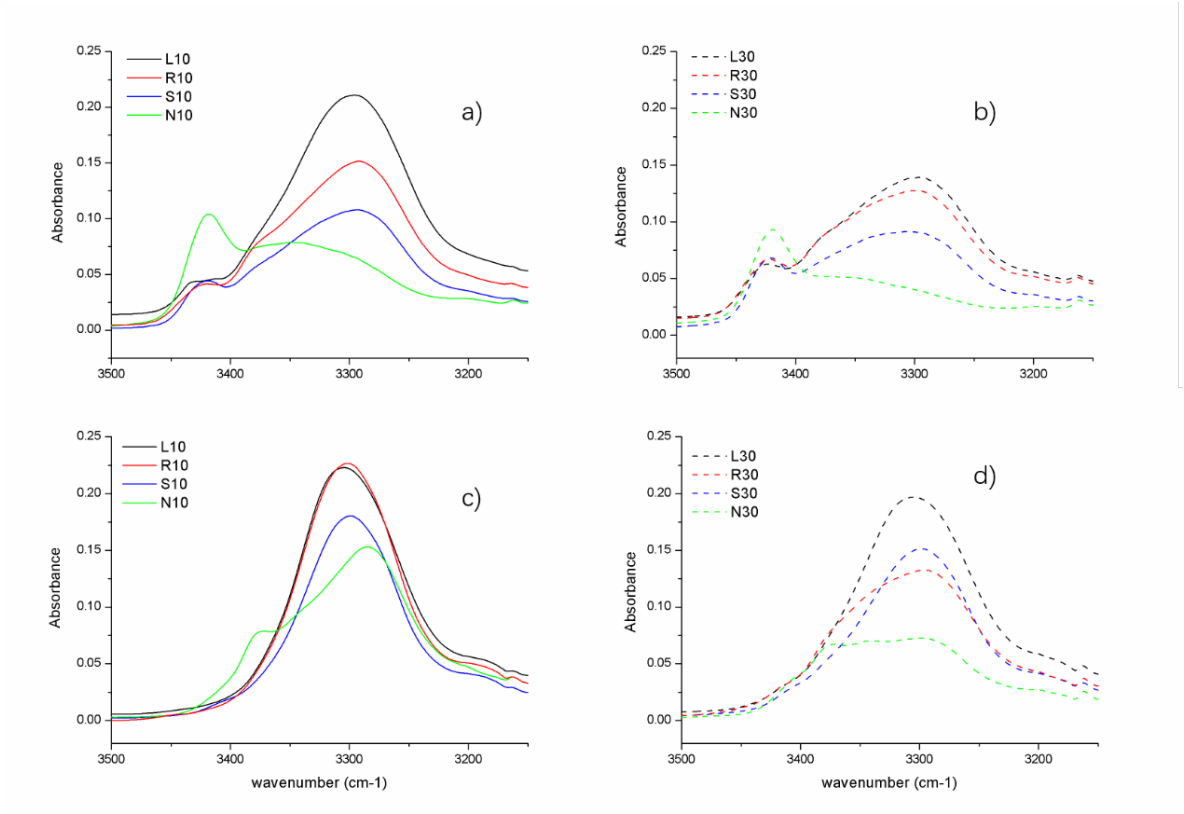

Figure 2. FTIR spectra of L_x, R_x, S_x and N_x at 2.8 mmol/L in chloroform (a, b) or toluene (c, d) for x = 10 (a, c) or 30 (b, d) (20°C).

The free NH band is however still present in chloroform even for L_{10}, R_{10} and S_{10} that self-assemble the most strongly. The number of molecules constituting one aggregate (*i.e.* the aggregation number, N_{agg}) should consequently be rather low in this solvent; which is not compatible with the formation of long nanorods. All polymers were therefore studied in a less polar solvent (toluene) to enhance the self-assembly of bis(urea)s compared to chloroform.[34] In toluene, only the broad stretching band of intermolecularly hydrogen bonded NH is observed for L_{10}, S_{10} and R_{10}, suggesting a very strong extent of aggregation at 20°C (Figure 2c), but also at higher temperatures

(Figure S7). On the contrary, the NH band broadens towards higher wavenumbers for N_{10}, R_{30} and N_{30} (and to a lesser extent for L_{30} and S_{30}), indicating a significantly lower extent of aggregation (Figures 2c,d). The FTIR experiments in toluene qualitatively confirm the conclusions of the experiments in chloroform and hint at a very strong assembly for L_{10}, R_{10} and S_{10}. All polymers were therefore studied by light and neutron scattering in toluene to gain further insight on the influence of the spacer on the assembly of tris(urea)s decorated by short PS arms.

Light and neutron scattering investigation of the self-assembly in toluene. The self-assembly of the polymers was studied by static (SLS) and dynamic (DLS) light scattering (LS) in toluene combined with small angle neutron scattering (SANS) in toluene-d_8. The solutions were prepared by direct dissolution of the polymers in toluene at room temperature. No significant evolution of the LS data at 20°C was observed after heating the solutions for one hour at 50°C (see SI section 2.3. for details) contrary to what was previously reported for PIB-decorated tris(urea)s,[24] implying that steady-state is reached rapidly at room temperature. LS studies were conducted at 1 g/L for L_{10}, S_{10}, R_{10}, L_{30} and S_{30}, which scattered light the most strongly, and at 10 g/L for the other polymers to afford a sufficiently strong scattering intensity. It was checked that in all cases interactions between the scatterers could be neglected (see SI section 2.2. for details) so that the form factor was directly measured. SANS experiments were conducted at ~10 g/L in all cases to allow reasonable measurement times. SLS and SANS data could be combined into a single set of data for each sample (see Figure 3 and SI section 2.4. for details). For most polymers, only one population of scatterers was identified based on DLS, SLS and SANS experiments. Only S_{30} and S_{10} showed a more complex behavior (see details below and in SI section 2.4.).

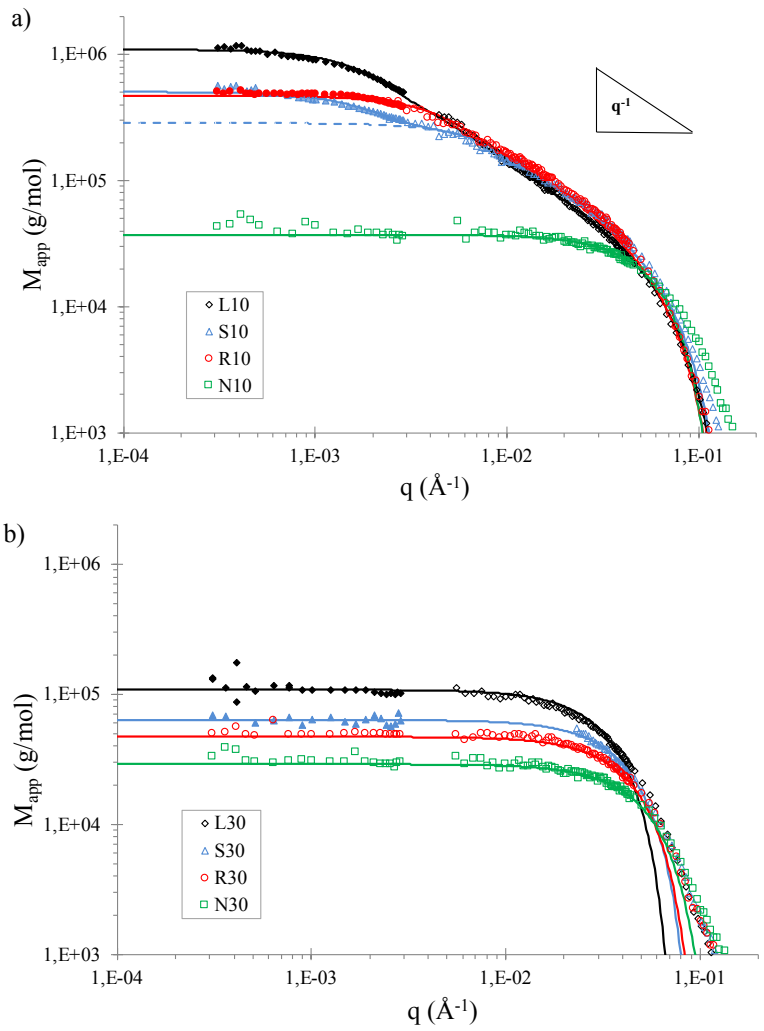

Figure 3. Evolution of the normalized scattered intensity M_{app} = I/KC versus the scattering vector (q) for solutions in toluene (SLS) or toluene-d_8 (SANS), measured at 1 g/L (full symbols) or 10 g/L (hollow symbols), for L_x (black diamonds), R_x (red circles), S_x (blue triangles), N_x (green squares). a) x = 10, b) x = 30. The lines correspond to fits according to models and parameters summarized in Tables 2 and 3. S_{10} contained a small amount of large aggregates which were either taken into account (solid line) or not (dashed line) in fitting the experimental data (see text).

The influence of the degree of polymerization (x) on the self-assembly of the polymers for a given spacer (and sticker) was first studied in order to know to which extent the small differences of molar mass and dispersities of the PS arms between the four series should be taken into account.

For all eight macromolecules, the normalized scattered intensity (I/KC) reached a plateau at the lowest q-values investigated, which corresponds to the weight-average molecular weight (M_w) of the assemblies. For x ~ 30, M_w was always low no matter the spacer, with an aggregation number ($N_{agg} = M_w/M_{w,unimer}$) lower than 15 for the four polymers (Table 2). Consistently, the scatterers were small according to their hydrodynamic radius determined by DLS (see Table 2) and to the fact that the scattered intensity was q-independent up to q ~ 2.10^{-2} Å^{-1} (see Figure 3b). The combined SLS and SANS data could be fitted well with a model of small monodisperse spherical particles (see SI section 2.4.c.). For x ~ 10, all polymers except N_{10} exhibited large N_{agg} and R_h (Tables 2 and 3, Figure 3a). Accordingly, the scattered intensity was already q-dependent at q ~ 2.10^{-3} Å^{-1}, confirming their large size. The drastic increase of the extent of self-assembly observed by the scattering experiments for L_x, R_x and S_x when x was decreased from ~ 30 to ~ 10 is consistent with the conclusions drawn from the FTIR experiments and is in agreement with previous theoretical[35] and experimental[26-29] studies.

Table 2. Characteristics of the spheres formed by N_{10}, L_{30}, R_{30}, S_{30} and N_{30} in toluene.

Polymer	R_h[a] (nm)	M_w [b] (kg/mol)	N_{agg}[c]	r^{fit} [d] (nm)
N_{10}	4	36	10	3.5
L_{30}	8	110	14	6.0
R_{30}	5	48	5	4.5
S_{30}	6	61	7	4.8
N_{30}	4	30	4	3.8

[a] From DLS. [b] M_w of the self-assembled particles deduced from the value of the plateau at low q in Figure 3. [c] $N_{agg} = M_w/M_{w,unimer}$ was calculated using $M_{w,unimer} = M_{n,NMR} \times Đ_{SEC}$. [d] The radius ($r^{fit}$) of the spheres was estimated by fitting the data with a model of monodisperse homogeneous spheres (see SI section 2.4.c.).

Table 3. Characteristics of the rods formed by L_{10}, R_{10} and S_{10} in toluene.

Polymer	R_h[a] (nm)	L^{DLS}[b] (nm)	M_w[c] (kg/mol)	N_{agg}[d]	L^{fit}[e] (nm)	r^{fit}[e] (nm)	M_L[e] ($kg.mol^{-1}.nm^{-1}$)	n_{cs}[f]
L_{10}	31	230	1100	330	230	2.6	4.6	0.6
R_{10}	17	90	470	110	85	2.8	5.4	0.6
S_{10}[g]	22	140	290	80	50	2.6	5.2	0.7

[a] Hydrodynamic radius obtained from DLS. [b] Length of the rods obtained from DLS (see SI section 2.1). For S_{10}, R_h (and therefore L^{DLS}) was overestimated because of the presence of spurious aggregates mentioned in the text. [c] Molar mass of the self-assembled particles deduced from the height of the plateau at low q in Figure 3. [d] $N_{agg} = M_w/M_{w,unimer}$ was calculated using $M_{w,unimer} = M_{n,NMR} \times Đ_{SEC}$. [e] The length ($L^{fit}$), radius ($r^{fit}$) and mass per unit length (M_L) of the rods were estimated by fitting the data with a model of monodisperse homogeneous rods (see SI section 2.4.b). [f] The number n_{cs} of molecules in the cross-section of the rods was deduced from M_L as follows: $n_{cs} = M_L \times e/M_{w,unimer}$ assuming a distance e = 0.46 nm between each hydrogen-bonded tris(urea). [g] The values given for S_{10} correspond to the population of rods only (dashed line on Figures 3a and 4), see text.

The self-assembly of the polymers with x ~ 10 was investigated in more detail. According to the value of the plateau of I/KC = f(q) at low q, the extent of aggregation followed the order $L_{10} > R_{10} \sim S_{10} >> N_{10}$ (see Figure 3 and Tables 2 and 3). This plateau for S_{10} is actually close to that of R_{10}, but this is due to the presence of a small amount of large aggregates (see explanations below and in SI section 2.4.b.). N_{10}, which is weakly aggregated in toluene, forms small particles the scattering of which is well described by a model of monodisperse spheres. On the contrary, solutions of L_{10}, S_{10} and R_{10} exhibit a q^{-1}-dependency of the scattered intensity in part of the q-range investigated by light and neutron scattering, which is characteristic of the formation of cylindrical particles (Figure 3a). Figure 4 reveals even more clearly the q-region where the scattered intensity is q^{-1}-dependent. From this figure, it appears that the length of the rods

(corresponding to the minimum value of q where I exhibits a q^{-1}-dependency) follows the order: $L_{10} > R_{10} \sim S_{10}$, which is consistent with the evolution of the aggregation number of these three polymers.

To deduce more quantitative information from the scattering experiments, the SLS and SANS data were fitted with a model of monodisperse homogeneous rods[33] (see SI section 2.4.b, Figures 3 and 4 and Table 3). The experimental data could be fitted well with this model for L_{10} and R_{10}. On the contrary, the low q region of S_{10} could not be fitted fully with a model of homogeneous rods (dashed blue line in Figures 3a and 4), even if a large polydispersity in length was included (data not shown). For this polymer, correct fitting was achieved by considering that the solution contained a small proportion of large aggregates in addition to monodisperse homogeneous rods (solid blue line on Figures 3a and 4). The R_h of the assemblies was moreover determined from the DLS data and used to calculate the length of the rods (L^{DLS}) for L_{10}, R_{10} and S_{10} (see Table 3 and SI section 2.1). The values of L^{DLS} are in very good agreement with those derived from the fit of the SLS/SANS (L^{fit}) for L_{10} and R_{10}, confirming the validity of the treatment. On the contrary, for S_{10} L^{DLS} was much larger than L^{fit} which was attributed to the presence of the large aggregates already mentioned resulting in an overestimation of R_h. The results summarized in Table 3 confirmed the qualitative observations discussed above that the extent of aggregation and length of the nanorods decrease in the order $L_{10} > R_{10} > S_{10} >> N_{10}$. The radius of the rods was similar for L_{10}, R_{10} and S_{10}, which is expected since this parameter is mainly controlled by the DP_n of the arms and their stretching.

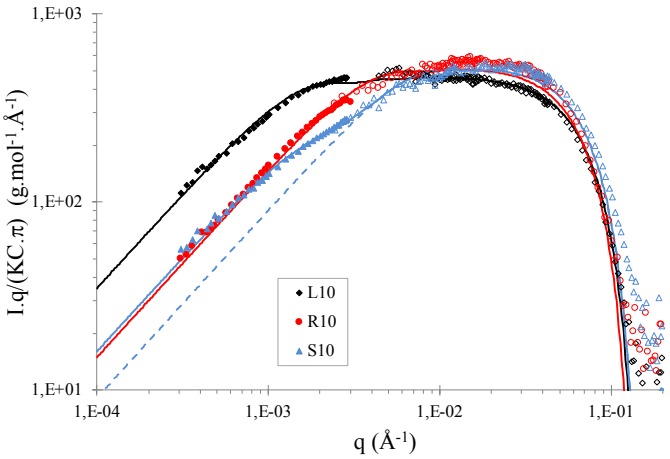

Figure 4. Normalized scattered intensity multiplied by q ($I \times q/\pi KC$) versus scattering vector (q) for solutions in toluene (SLS) or toluene-d_8 (SANS) measured at 1g/L (hollow symbols) or 10g/L (full symbols) for L_{10} (black diamonds), R_{10} (red circles) and S_{10} (blue triangles). S_{10} contained a small amount of large aggregates which were either taken into account (solid line) or not (dashed line) in fitting the experimental data.

Finally, for the three polymers leading to cylindrical particles (L_{10}, R_{10} and S_{10}), the molecular weight per unit length of the rods (M_L) could be determined from the q^{-1}-dependent region (see SI section 2.4.b. for details and Table 3). Taking into account that the distance between two successive hydrogen-bonded ureas is 0.46 nm,[36] the values of M_L indicate that approximately one molecule is present in the cross-section of the self-assembled rods for these three systems. This is consistent with a model of self-assembly where the tris(urea)s stack one atop the other in the direction of the rod[37] (Figure 5).

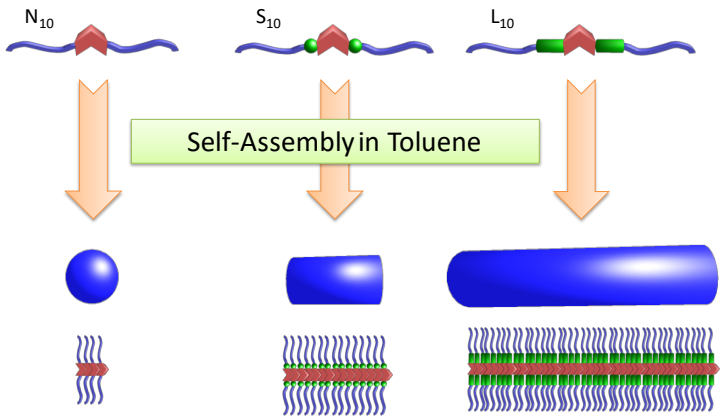

Figure 5. Schematic representation of the influence of the spacer on the self-assembly of PS-functionalized tris(urea)s assembling by 1D stacking through cooperative hydrogen bonding.

The results gathered from FTIR, SLS and SANS experiments in toluene for x ~ 10 confirm that the extent of aggregation strongly increases by separating the tris(urea) self-assembling sticker from the PS arms with a spacer, leading to long and rigid nanorods for L_{10}, R_{10} and S_{10}, whereas N_{10} forms weakly aggregated spherical particles. This is in agreement with the fact that moving away the styrene units from the tris(urea) reduces steric hindrance and favors hydrogen bonding. As discussed below, this result can only be explained by a change of the spacer and not by a difference of molar mass or molar mass distribution of the PS arms.

Furthermore, significant differences were observed according to the type of spacer: the length of the rods varies in the order $L_{10} > R_{10} > S_{10}$. L_{10} and S_{10} possess PS arms of very similar molar mass distributions (Figure 1, Table 1), which allows comparing the effect of the spacer independently from the molar mass of the arms. The fact that the length of the rods formed by L_{10} is much larger than that of S_{10} is in agreement with the idea that reducing steric hindrance close to the tris(urea) sticker favors self-assembly. With this in mind, it could be expected that R_{10}, containing an even longer spacer than L_{10}, would form the longest assemblies. However, even though R_{10} does form slightly longer structures than S_{10}, it does not self-assemble as strongly as L_{10}. R_{10} has a different

molar mass distribution compared to L_{10}, but this cannot account for the observed results. Indeed, the major difference between both polymers is the presence of a significant amount of longer PS arms for L_{10}, which should favor the formation of shorter structures for L_{10} contrary to what is observed. We propose that the trithiocarbonate moiety in R_{10} imposes a conformation to the spacer that is more sterically demanding than a simple alkyl chain, resulting in an overall weaker, *i.e.* shorter, assembly.

CONCLUSION

Four spacers of different lengths were used to link a tris(urea) sticker to PS arms. When the PS arms had a degree of polymerization x ~ 30, their entropic penalty of stretching strongly limited self-assembly in toluene. As a consequence, although the spacer did have a small influence on the extent of self-assembly ($L_{30} > S_{30} \sim R_{30} > N_{30}$), weakly aggregated spherical particles were formed, no matter the spacer. On the contrary, for shorter arms (x ~ 10), the extent of aggregation strongly increased by separating the tris(urea) sticker from the PS arms with a spacer, leading to long and rigid nanorods for L_{10}, R_{10} and S_{10} contrary to N_{10}. This indicates that moving away the styrene units from the tris(urea) reduces steric hindrance and favors hydrogen bonding. Efficient control of the length of the rods could be achieved by varying the nature of the spacer: L_{10} (with a 9 atom spacer) forms 5 times longer rods than S_{10} (with a 5 atom spacer). These results reveal the possibility to tune the length of supramolecular nanorods decorated by polymer chains with minimal modification of the building block, *i.e.* without affecting the radius or the functionality of the rods. The trends demonstrated in the case of polystyrene arms certainly apply qualitatively to other polymers with the caveat that the influence of the spacer is expected to be exacerbated by the bulkiness of the monomer. With this approach, the role of the length of the rods on their

functional properties (stabilization of emulsions, optical properties, rheological properties...) can be investigated independently of any other parameter.

ASSOCIATED CONTENT

Supporting Information. Synthesis and additional scattering data.

AUTHOR INFORMATION

Corresponding Authors

* E-mail: Olivier.Colombani@univ-lemans.fr (O.C.), laurent.bouteiller@upmc.fr (L.B.)

ACKNOWLEDGMENT

S.H. acknowledges financial support from the China Scholarship Council. M. Detrez (LLB, Saclay) and G. Pembouong (IPCM, Paris) are acknowledged for assistance with SANS and SEC measurements, respectively.

REFERENCES

(1) Hu, J.; Odom, T. W.; Lieber, C. M. Chemistry and Physics in One Dimension: Synthesis and Properties of Nanowires and Nanotubes. *Acc. Chem. Res.* **1999**, *32* (5), 435–445.

(2) Wang, F.; Dong, A.; Buhro, W. E. Solution–Liquid–Solid Synthesis, Properties, and Applications of One-Dimensional Colloidal Semiconductor Nanorods and Nanowires. *Chem. Rev.* **2016**, *116* (18), 10888–10933.

(3) Aravindan, V.; Sennu, P.; Lee, Y.-S.; Madhavi, S. Practical Li-Ion Battery Assembly with One-Dimensional Active Materials. *J. Phys. Chem. Lett.* **2017**, *8* (17), 4031–4037.

(4) Alim, S.; Vejayan, J.; Yusoff, M. M.; Kafi, A. K. M. Recent Uses of Carbon Nanotubes & Gold Nanoparticles in Electrochemistry with Application in Biosensing: A Review. *Biosensors and Bioelectronics* **2018**, *121*, 125–136.

(5) Brea, R. J.; Reiriz, C.; Granja, J. R. Towards Functional Bionanomaterials Based on Self-Assembling Cyclic Peptide Nanotubes. *Chem. Soc. Rev.* **2010**, *39* (5), 1448–1456.

(6) Raynal, M.; Portier, F.; van Leeuwen, P. W. N. M.; Bouteiller, L. Tunable Asymmetric Catalysis through Ligand Stacking in Chiral Rigid Rods. *J. Am. Chem. Soc.* **2013**, *135* (47), 17687–

17690.

(7) Desmarchelier, A.; Caumes, X.; Raynal, M.; Vidal-Ferran, A.; van Leeuwen, P. W. N. M.; Bouteiller, L. Correlation between the Selectivity and the Structure of an Asymmetric Catalyst Built on a Chirally Amplified Supramolecular Helical Scaffold. *J. Am. Chem. Soc.* **2016**, *138*, 4908–4916.

(8) Courtois, J.; Baroudi, I.; Nouvel, N.; Degrandi, E.; Pensec, S.; Ducouret, G.; Chaneac, C.; Bouteiller, L.; Creton, C. Supramolecular Soft Adhesive Materials. *Adv. Funct. Mater.* **2010**, *20* (11), 1803–1811.

(9) Murphy, C. J.; Sau, T. K.; Gole, A. M.; Orendorff, C. J.; Gao, J.; Gou, L.; Hunyadi, S. E.; Li, T. Anisotropic Metal Nanoparticles: Synthesis, Assembly, and Optical Applications. *J. Phys. Chem. B* **2005**, *109* (29), 13857–13870.

(10) Niekiel, F.; Spiecker, E.; Bitzek, E. Influence of Anisotropic Elasticity on the Mechanical Properties of Fivefold Twinned Nanowires. *J. Mech. Phys. Solids* **2015**, *84*, 358–379.

(11) Gantenbein, D.; Schoelkopf, J.; Matthews, G. P.; Gane, P. A. C. Determining the Size Distribution-Defined Aspect Ratio of Rod-like Particles. *Applied Clay Science* **2011**, *53* (4), 538–543.

(12) Khoo, I.-C. *Liquid Crystals*; John Wiley & Sons, 2007; Vol. 64.

(13) Hartgerink, J.; Zubarev, E. R.; Stupp, S. I. Supramolecular One-Dimensional Objects. *Current Opinion in Solid State and Materials Science* **2001**, *5* (4), 355–361.

(14) Palmer, L. C.; Stupp, S. I. Molecular Self-Assembly into One-Dimensional Nanostructures. *Acc. Chem. Res.* **2008**, *41* (12), 1674–1684.

(15) Kim, S.; Kim, J. H.; Lee, J. S.; Park, C. B. Beta-Sheet-Forming, Self-Assembled Peptide Nanomaterials towards Optical, Energy, and Healthcare Applications. *Small* **2015**, *11* (30), 3623–3640.

(16) Couet, J.; Biesalski, M. Surface-Initiated ATRP of *N* -Isopropylacrylamide from Initiator-Modified Self-Assembled Peptide Nanotubes. *Macromolecules* **2006**, *39* (21), 7258–7268.

(17) Couet, J.; Biesalski, M. Polymer-Wrapped Peptide Nanotubes: Peptide-Grafted Polymer Mass Impacts Length and Diameter. *Small* **2008**, *4* (7), 1008–1016.

(18) Chapman, R.; Koh, M. L.; Warr, G. G.; Jolliffe, K. A.; Perrier, S. Structure Elucidation and Control of Cyclic Peptide-Derived Nanotube Assemblies in Solution. *Chem. Sci.* **2013**, *4* (6), 2581.

(19) Chapman, R.; Jolliffe, K. A.; Perrier, S. Multi-Shell Soft Nanotubes from Cyclic Peptide Templates. *Adv. Mater.* **2013**, *25* (8), 1170–1172.

(20) Seoudi, R. S.; Del Borgo, M. P.; Kulkarni, K.; Perlmutter, P.; Aguilar, M.-I.; Mechler, A. Supramolecular Self-Assembly of 14-Helical Nanorods with Tunable Linear and Dendritic Hierarchical Morphologies. *New J. Chem.* **2015**, *39* (5), 3280–3287.

(21) Li, W.; Che, X.; Chen, F.; Zhang, C.; Zhang, T.; Wang, H.; Bai, B.; Li, M. Observation of Morphology and Structure Evolution during Gelation of a Bis(Anhydrazide) Derivative. *J. Phys. Chem. B* **2017**, *121* (37), 8795–8801.

(22) Silk, M. R.; Mohanty, B.; Sampson, J. B.; Scanlon, M. J.; Thompson, P. E.; Chalmers, D. K. Controlled Construction of Cyclic D/L Peptide Nanorods. *Angew. Chem. Int. Ed.* **2019**, *58* (2), 596–601.

(23) Knoben, W.; Besseling, N. A. M.; Bouteiller, L.; Stuart, A. C. Dynamics of Reversible Supramolecular Polymers: Independent Determination of the Dependence of Linear Viscoelasticity on Concentration and Chain Length by Using Chain Stoppers. *Phys. Chem. Chem. Phys.* **2005**, *7* (11), 2390–2398.

(24) Catrouillet, S.; Fonteneau, C.; Bouteiller, L.; Delorme, N.; Nicol, E.; Nicolai, T.; Pensec, S.; Colombani, O. Competition Between Steric Hindrance and Hydrogen Bonding in the Formation of Supramolecular Bottle Brush Polymers. *Macromolecules* **2013**, *46* (19), 7911–7919.

(25) Han, S.; Nicol, E.; Niepceron, F.; Colombani, O.; Pensec, S.; Bouteiller, L. Oligo-Urea with No Alkylene Unit Self-Assembles into Rod-like Objects in Water. *Macromol. Rapid Commun.* **2019**, 1800698.

(26) Catrouillet, S.; Bouteiller, L.; Nicol, E.; Nicolai, T.; Pensec, S.; Jacquette, B.; Le Bohec, M.; Colombani, O. Self-Assembly and Critical Solubility Temperature of Supramolecular Polystyrene Bottle-Brushes in Cyclohexane. *Macromolecules* **2015**, *48*, 1364–1370.

(27) Catrouillet, S.; Brendel, J. C.; Larnaudie, S.; Barlow, T.; Jolliffe, K. A.; Perrier, S. Tunable Length of Cyclic Peptide–Polymer Conjugate Self-Assemblies in Water. *ACS Macro Letters* **2016**, *5* (10), 1119–1123.

(28) Chapman, R.; Warr, G. G.; Perrier, S.; Jolliffe, K. A. Water-Soluble and PH-Responsive Polymeric Nanotubes from Cyclic Peptide Templates. *Chemistry - A European Journal* **2013**, *19* (6), 1955–1961.

(29) Larnaudie, S. C.; Brendel, J. C.; Jolliffe, K. A.; Perrier, S. pH-Responsive, Amphiphilic Core–Shell Supramolecular Polymer Brushes from Cyclic Peptide–Polymer Conjugates. *ACS Macro Letters* **2017**, *6* (12), 1347–1351.

(30) Dong, S.; Zhao, W.; Lucien, F. P.; Perrier, S.; Zetterlund, P. B. Polymerization Induced Self-Assembly: Tuning of Nano-Object Morphology by Use of CO_2. *Polym. Chem.* **2015**, *6* (12), 2249–2254.

(31) Mellot, G.; Guigner, J.-M.; Jestin, J.; Bouteiller, L.; Stoffelbach, F.; Rieger, J. Bisurea-Functionalized RAFT Agent: A Straightforward and Versatile Tool toward the Preparation of Supramolecular Cylindrical Nanostructures in Water. *Macromolecules* **2018**, *51* (24), 10214–10222.

(32) Fonteneau, C.; Pensec, S.; Bouteiller, L. Versatile Synthesis of Reversible Comb-Shaped Supramolecular Polymers. *Polym. Chem.* **2014**, *5* (7), 2496–2505.

(33) SasView: http://www.sasview.org/.

(34) Simic, V.; Bouteiller, L.; Jalabert, M. Highly Cooperative Formation of Bis-Urea Based Supramolecular Polymers. *J. Am. Chem. Soc.* **2003**, *125* (43), 13148–13154.

(35) Wang, Z.; Safran, S. A. Size Distribution for Aggregates of Associating Polymers. II. Linear Packing. *J. Chem. Phys.* **1988**, *89* (8), 5323–5328.

(36) Pérez-Folch, J.; Subirana, J. A.; Aymami, J. Polar Structure of N,N′-Dimethylurea Crystals. *J. Chem. Crystallogr.* **1997**, *27* (6), 367–369.

(37) Brocorens, P.; Linares, M.; Guyard-Duhayon, C.; Guillot, R.; Andrioletti, B.; Suhr, D.; Isare, B.; Lazzaroni, R.; Bouteiller, L. Conformational Plasticity of Hydrogen Bonded Bis-Urea Supramolecular Polymers. *J. Phys. Chem. B* **2013**, *117* (17), 5379–5386.

for Table of Contents use only